Creative Commons Attribution

Periodica Polytechnica Civil Engineering, 70(1), pp. 244–255, 2026

Comparative Analysis of the Numerical Model and Geodetic Measurements of the Settlement in the Kobilja Glava Tunnel

Satko Filipović[1*], Ekrem Bektašević[2], Žanesa Ljevo[3], Kemal Gutić[2]

[1] Directorate for Roads of Sarajevo Canton, Hamida Dizdara 1., 71000 Sarajevo, Bosnia and Herzegovina
[2] Faculty of Mining, Geology and Civil Engineering, University of Tuzla, Urfeta Vejzagića 2., 75000 Tuzla, Bosnia and Herzegovina
[3] Faculty of Civil Engineering, University of Sarajevo, Patriotske lige 30., 71000 Sarajevo, Bosnia and Herzegovina
* Corresponding author, e-mail: satko.filipovic@gmail.com

Received: 01 December 2025, Accepted: 14 February 2026, Published online: 05 March 2026

Abstract

This paper presents a comparative analysis of the settlement of the Kobilja Glava tunnel structure, using three-dimensional numerical modeling and geodetic monitoring during construction. The numerical model, developed in the Plaxis 3D software package, included all excavation and support phases, with rock mass parameters defined based on RMR classification and conversion of Hoek-Brown parameters into the Mohr-Coulomb form. The primary lining was modeled using plate elements, while anchors were represented as embedded elements with equivalent elastic modulus.

Geodetic measurements were carried out continuously, with measurement points positioned at the tunnel crown, sidewalls, and the bench, providing actual convergence values. Comparison between the numerical model results and geodetic measurements revealed discrepancies ranging from 18% to 24%, with the largest deviations recorded at a distance of 24 m from the excavation face. Statistical data analysis (RMSE ≈ 3.71 mm; $\sigma \approx 1.21$ mm) confirmed the presence of a systematic prediction error, but also the stability of deviations across the analyzed points.

The results confirm the technical validity of the applied model and the designed support system, while emphasizing the need for dynamic updating of numerical models in accordance with field data. This further reinforces the implementation of the observational method as a reliable approach under real tunneling conditions.

Keywords

numerical modeling, Plaxis 3D, geodetic measurements, tunnel settlement, convergence

1 Introduction

The rapid development of urban areas in recent decades has contributed to the growing need for the utilization of underground space. Tunnels are considered an efficient solution for overcoming congestion problems and reducing traffic pressure [1, 2]. Tunnel excavation represents an extremely demanding and comprehensive engineering activity [3, 4], primarily based on geotechnical and geophysical investigations that are closely linked to the planned excavation methods and support systems. In this context, the application of seismic refraction for determining geomechanical parameters [5], as well as the multichannel analysis of surface waves (MASW) within shallow geophysical investigations [6], has proven to be a reliable approach for rock mass characterization in the excavation zone. The selection of an appropriate tunneling procedure for large-span tunnels in soft ground is a key factor for successful construction [7–9]. The Kobilja Glava tunnel forms part of the main project connecting Vogošća with Sarajevo, providing a link between the city center of Sarajevo and the A1 motorway on Corridor Vc.

The project design specifies a twin-tube tunnel, with each individual tube designated for one direction of traffic. The axial distance between the tunnel tubes is 25 m. The Kobilja Glava tunnel was excavated beneath the hill of the same name in the city of Sarajevo Fig. 1 [10]. Approximately 500 residential units are located above the tunnel, and in order to prevent potential damage to these structures, it was necessary to carefully monitor tunnel convergence during excavation.

The New Austrian Tunneling Method (NATM) was applied in the construction of the Kobilja Glava tunnel. For the purpose of timely monitoring of convergence,

Cite this article as: Filipović, S., Bektašević, E., Ljevo, Ž., Gutić, K. "Comparative Analysis of the Numerical Model and Geodetic Measurements of the Settlement in the Kobilja Glava Tunnel", Periodica Polytechnica Civil Engineering, 70(1), pp. 244–255, 2026. https://doi.org/10.3311/PPci.42928

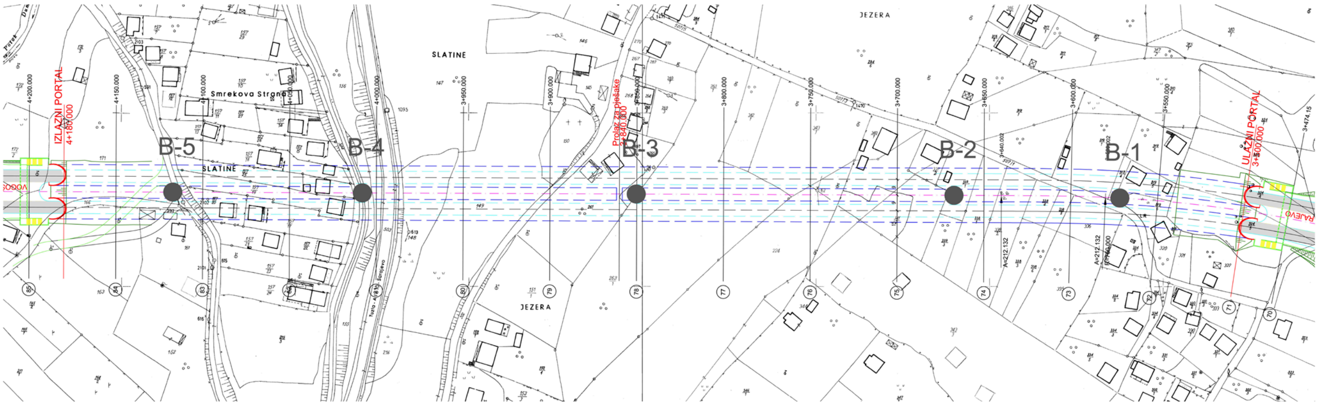

Fig. 1 Layout of the Kobilja Glava Tunnel [10]

two independent methods were implemented. The first involved the development of a numerical model (3D model) capable of simulating soil and rock mass behavior using various constitutive models. The numerical model covered all stages of tunnel construction, thus simulating the actual construction process [11]. The Plaxis 3D software package [12] was used for model development, enabling the estimation of expected convergence values.

The second method consisted of continuous geodetic monitoring during excavation, providing actual convergence values. Based on the collected data, it was possible to make the necessary corrections both in the construction methodology and in the support system itself.

The total length of the right tunnel tube is 635.10 m, of which 587.10 m is underground excavation. The temporary entrance portal of the right tube is located at station 3 + 550.15, while the temporary exit portal is at station 4 + 137.15 (stations measured along the right tunnel axis). The left tunnel tube has a total length of 638.885 m, with an excavation length of 590.885 m. The temporary entrance portal of the left tunnel tube is located at station 3 + 546.952, and the temporary exit portal is at 4 + 128.09 (along the left tunnel axis). Due to the significant longitudinal gradient of the tunnel, the main design defined two cross-passages connecting the left and right tunnel tubes [13].

By comparing the results obtained from the numerical model in Plaxis 3D [12] with those obtained from continuous geodetic monitoring, the aim was to demonstrate the importance of the observational method, i.e., combining these two approaches to obtain an accurate representation of tunnel convergence during construction.

2 Numerical modeling

In the tunnel design phase, the accurate development of a computational model is of great importance, with the objective of predicting the behavior of a complex system consisting of the tunnel structure and the surrounding ground/rock mass [14–16]. Considering this, it is essential that numerical modeling realistically represents the processes occurring within the tunnel structure and its surrounding medium as a complex interactive system during construction.

When analyzing the interaction between the tunnel lining and the surrounding medium, it is important to emphasize that, at the time the lining is formed, it is not influenced by the stress–strain changes that have already occurred in the surrounding rock mass. This means that the shotcrete lining is exposed only to the displacements of the excavation contour that occur after its installation [17]. As a result, for reliable analysis of the stress–strain state within the rock mass and tunnel structure, it is crucial to consider the partial relaxation of the surrounding medium, i.e., the deformations of the excavation contour that occur before lining placement.

In this context, seismic methods for determining the depth of the rock mass damage zone [18, 19] can also be applied in cases without blasting, serving as an additional tool for accurate characterization of the deformability of the surrounding material and for validation of input parameters in numerical analyses. Therefore, a three-dimensional analysis is required to simulate the progress of excavation, stress changes, and deformations around the temporary excavation face.

In practice, however, the finite element method (FEM) in three-dimensional analysis is not commonly applied due to limited computational resources and design constraints. The use of 3D software is restricted by high costs and long analysis times, which is why it is often limited to complex, high-budget projects or research studies [20].

In engineering practice, 2D numerical models are predominantly used for practical reasons – they significantly reduce computational complexity and analysis time, allowing for faster decision-making while maintaining sufficient accuracy for many typical tasks and projects.

2.1 Details of the numerical model

2.1.1 Rock mass modeling

Modeling of the rock mass was carried out in three clearly defined steps:

1. Geological mapping and rock mass classification:
   Based on field investigations, geological mapping was conducted for the relevant tunnel section [21]. The RMR classification was used to define the basic parameters of the rock mass:
   - Cohesion (*c*) = 78 kPa;
   - Internal friction angle (*φ*) = 32°;
   - Elastic modulus (*E*) = 107,000 kPa.

   The analyzed section refers to the left tunnel tube between stations km 3 + 744.00 and km 3 + 824.00.
2. Parameterization in RocLab [22]:
   The obtained geological data were used to determine the input parameters of the rock mass using the RocLab software package [22–24]. Based on the Hoek-Brown model, the parameters were converted into Mohr-Coulomb form as follows: Implementation in Plaxis 3D [12].

The parameters derived in RocLab [22] were entered into Plaxis 3D [12] for the development of the three-dimensional numerical model. The model covered a 60 m-long segment, with a 23 m overburden above the tunnel crown. Boundary conditions were defined automatically in accordance with the software's standard rules.

The adopted terrain profile, shown in Fig. 2, consists of a 5 m thick layer of weathered overburden, underlain by a substrate of gray marl with a layered structure. The modeled section corresponds to a standard tunnel cross-section, 60 m in length. The overburden above the upper edge of the tunnel tube to the ground surface is 23 m. Regarding boundary conditions, Plaxis 3D [12] automatically generates a set of standard boundary constraints at the edges of the geometric model. These are defined according to the following rules:

- The vertical boundaries of the model with normals along the x-axis (parallel to the y–z plane) are fixed but free to move in the y and z directions.
- The vertical boundaries of the model with normals along the y-axis (parallel to the x–z plane) are fixed but free to move in the x and z directions.
- The bottom boundary of the model is fixed in all directions.

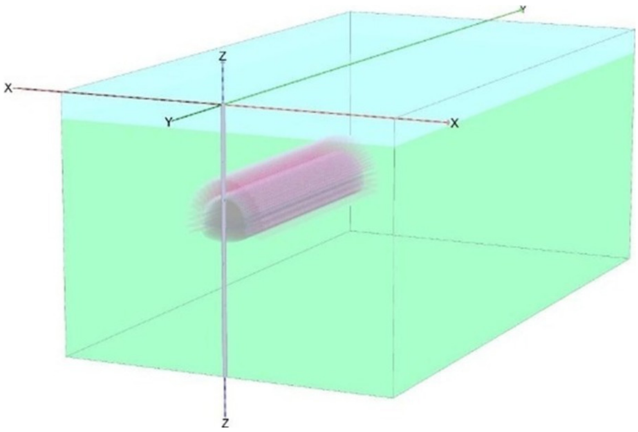

Fig. 2 Representation of rock material layers

2.1.2 Modeling of shotcrete

For modeling shotcrete, as one of the most important components of the tunnel's primary lining, the software package uses predefined plate elements [25, 26]. To define these plate elements, it is necessary to input the following parameters:

- Elastic modulus;
- Element thickness;
- Unit weight (density);
- Poisson's ratio.

The values entered into the model are presented in Table 1.

The time-dependent stiffness of shotcrete, as the term itself suggests, depends on the passage of time from the moment of installation until the designed concrete strength is achieved. In the Plaxis 3D software [12], it is possible to incorporate these effects by means of a user-defined curve through a table that accounts for the time-dependent values of the elastic modulus as well as the strength gain over a defined time interval. However, due to the complexity of the numerical model and the extremely long computation time, this effect was not considered in the present study.

2.1.3 Modeling of anchors

During the construction of the Kobilja Glava Tunnel, IBO anchors were predominantly used. The anchor

Table 1 Parameters used for modeling shotcrete

Characteristics	Designation	Value	Unit
Elastic modulus	*E*	15	GPa
Thickness	*d*	25	cm
Unit weight	*g*	25	kN/m^3
Poisson's ratio	*u*	0.2	–

lengths varied, and on the analyzed section, anchors with a length of 4 m were installed. In Plaxis 3D [12], anchors are modeled as embedded beam elements. These elements are designed to carry the following stresses: axial force, shear force, and bending moment.

For accurate modeling of an embedded beam element, it is necessary to define the elastic modulus, which, due to the installation technology (involving a cement grout injection), can only be represented as an equivalent elastic modulus. This is because the modulus must account for both the properties of the hardened cement grout and the steel used for the anchor bar. After the cement grout hardens, the cross-section effectively behaves as a composite section.

The equivalent elastic modulus of the anchor is obtained using the following formula (Eq. (1)):

$$E_{eq} = E_b \times \frac{A_b}{A} + E_s \times \frac{A_s}{A}, \quad (1)$$

where:

- E_b: elastic modulus of concrete;
- E_s: elastic modulus of steel;
- A: total cross-sectional area of the composite section;
- A_b: area of the concrete part of the composite section;
- A_s: area of the steel part of the composite section.

The given values in Eq. (1) can be seen in the following linsting:

- $E_b = 3 \times 10^7$ kPa;
- $E_s = 2.1 \times 10^8$ kPa;
- $A = 0.0020$ m^2;
- $A_b = 0.0014$ m^2;
- $A_s = 0.0005$ m^2.

By substituting these values into the above expression, the equivalent elastic modulus is obtained as:

$$E_{eq} = 73.5 \times 10^6 \text{ kPa}.$$

Once all of the above parameters were defined, the construction of the numerical model was initiated. The tunnel was positioned in accordance with the coordinate origin and the overburden thickness, as previously described.

Subsequently, the tunnel cross-section was defined. There are several ways to input the cross- section into the model:

- using the import option, which allows the cross-section previously defined in AutoCAD [27] to be imported into Plaxis 3D [12], or
- by defining the geometric characteristics of the tunnel lining segments directly within Plaxis 3D [12].

For the purposes of this model, the second method was used – the tunnel lining elements were defined directly in Plaxis 3D [12]. The representation of the tunnel lining cross-section in Plaxis 3D [12] is shown in Fig. 3.

The model shows a cross-section of the tunnel, clearly illustrating its division into two parts. The upper part represents the tunnel's crown (calotte), while the lower part represents the bench with a permanent invert. The boundary between these two parts actually represents a temporary invert, which is removed once the excavation of the bench begins.

The purpose of this temporary invert is to ensure that, in sections of the tunnel excavated in poor ground conditions, the lining ring is closed as quickly as possible. This allows for a more uniform redistribution of stresses and reduces the convergence that occurs due to the disturbance of the stress state in the rock mass during tunnel excavation.

After defining the geometry of the tunnel cross-section, the next step is to define the total tunnel length. In this particular case, the tunnel length was set to 60 m. When defining the length, it is also necessary to take into account the advance step of the tunnel crown, which, according to the geotechnical conditions for this section of the Kobilja Glava tunnel, was 1.2 m. Accordingly, the tunnel was divided into 50 excavation steps.

Each geometry line was then assigned the previously defined properties of the plate elements. After this, it was necessary to activate the negative interface option, in order to densify the finite element mesh at the contact between the shotcrete lining and the rock mass, so that this interface would exhibit the mechanical characteristics of the rock mass (Fig. 4).

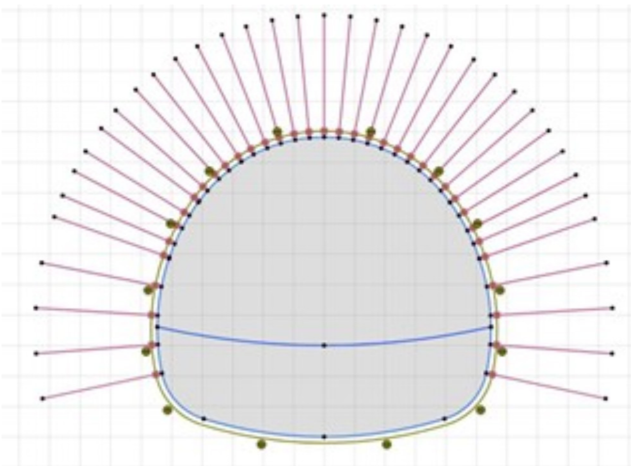

Fig. 3 Cross-sectional view of the tunnel lining with anchors from Plaxis 3D [12]

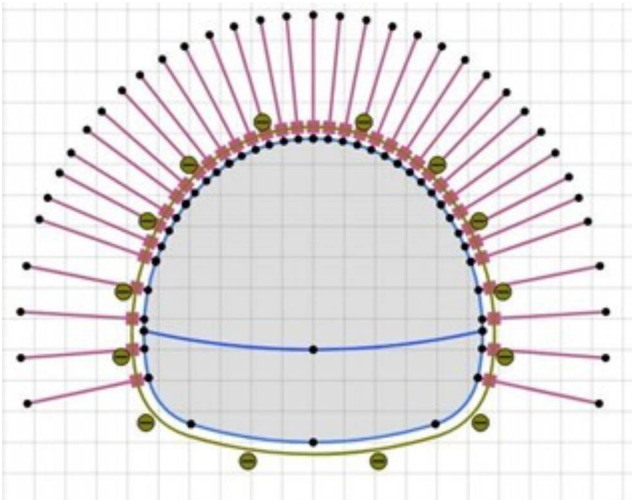

Fig. 4 Representation of a plate element with a negative interface

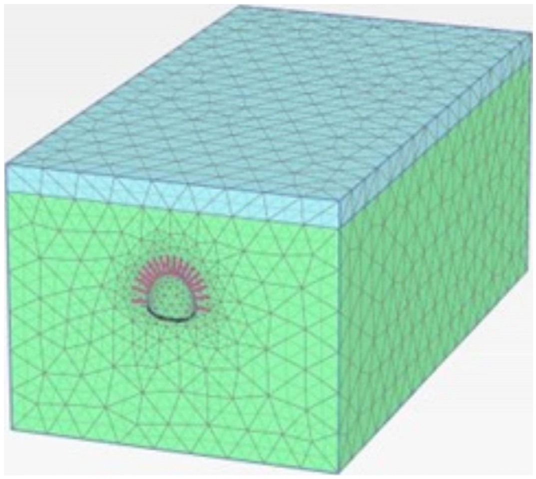

Fig. 6 Finite element mesh of the numerical model

The arrangement and positioning of the anchors in the model were fully defined in accordance with their layout specified in the geotechnical design documents.

Figs. 5 and 6 show the adopted computational model (Fig. 5), as well as the finite element mesh used within the numerical model (Fig. 6).

2.2 Geodetic measurements

During the excavation of the tunnel crown, the position of the excavation boundaries was continuously monitored using precise geodetic instruments such as total stations, laser scanners, or GNSS systems (when applicable). Regular measurements were conducted to verify the compliance of the excavation with the designed tunnel profile geometry, while all deviations were recorded and analyzed [28–30].

The use of these instruments enabled high accuracy in collecting convergence data, which, under poor rock mass conditions – classified as complex working conditions – were gathered on a daily basis.

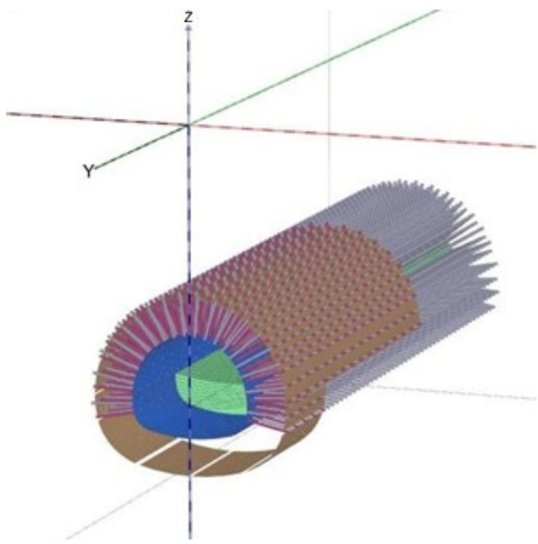

Fig. 5 Representation of the 3D numerical model of the tunnel

The typical positioning of measurement points (targets) within the tunnel profile involves placing one point at the highest position of the tunnel crown, and two additional points on the side walls of the crown section, symmetrically in relation to the first point. Additionally, one point is placed on the left and one on the right bench, respectively Fig. 7 [31].

3 Comparison of results – numerical model *vs*. geodetic measurements

Section 3 presents a comparative analysis of the results obtained using the numerical model developed in the Plaxis 3D software package [12] and the actual convergence values measured geodetically during tunnel construction [32–34].

For this purpose, a tunnel excavation length of 30 m was first defined, along with a reference point located at

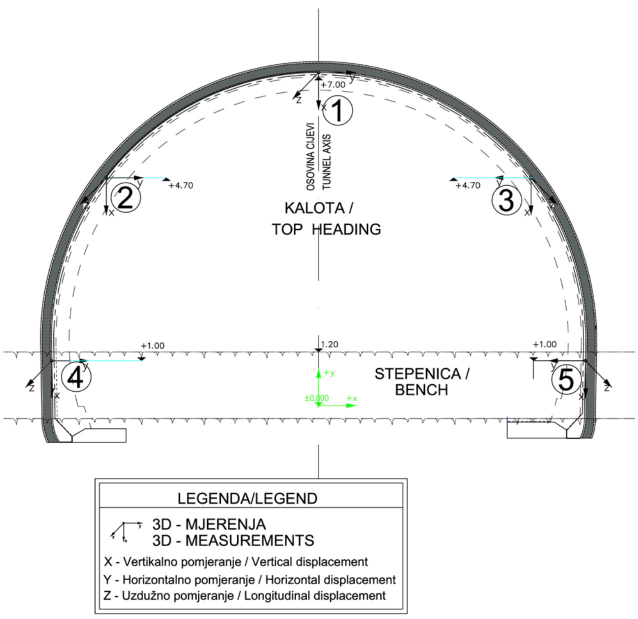

Fig. 7 Measurement points for monitoring tunnel convergence [31]

the crown of the tunnel cross-section, whose convergence was to be monitored. Subsequently, the tunnel excavation process was simulated, following the excavation and support installation sequences defined in the Geotechnical Design Mission. The excavation step length was set to 1.2 m, and the support elements used for excavation stabilization consisted of 25 cm of shotcrete, steel lattice girders, and Ø32 IBO anchors grouted with an injection mixture.

Furthermore, the distances between the excavation face and the observed point were defined for which the numerical model calculations were performed. Distances of 6 m, 12 m, and 24 m from the excavation face were analyzed, monitoring the deformation of the crown reference point. It is also important to emphasize that excavations were carried out for both the crown section and the bench with the permanent invert, thereby forming a closed ring around the excavation.

Figs. 8 to 10 show the settlement values of the crown point of the tunnel for the specified distances, as obtained from the numerical model. The closure of the excavation ring in the analyzed stages demonstrated a stabilizing effect on settlement, which is consistent with the expected behavior in weakly consolidated marl formations.

In order to validate the model itself, it was necessary to compare the obtained results with the theoretically established characteristic settlement values for marls, as reported in the literature. The diagram of Fig. 11 [35] shows the characteristic settlement values.

Independently of the numerical model, permanent geodetic surveys were carried out during the excavation of the

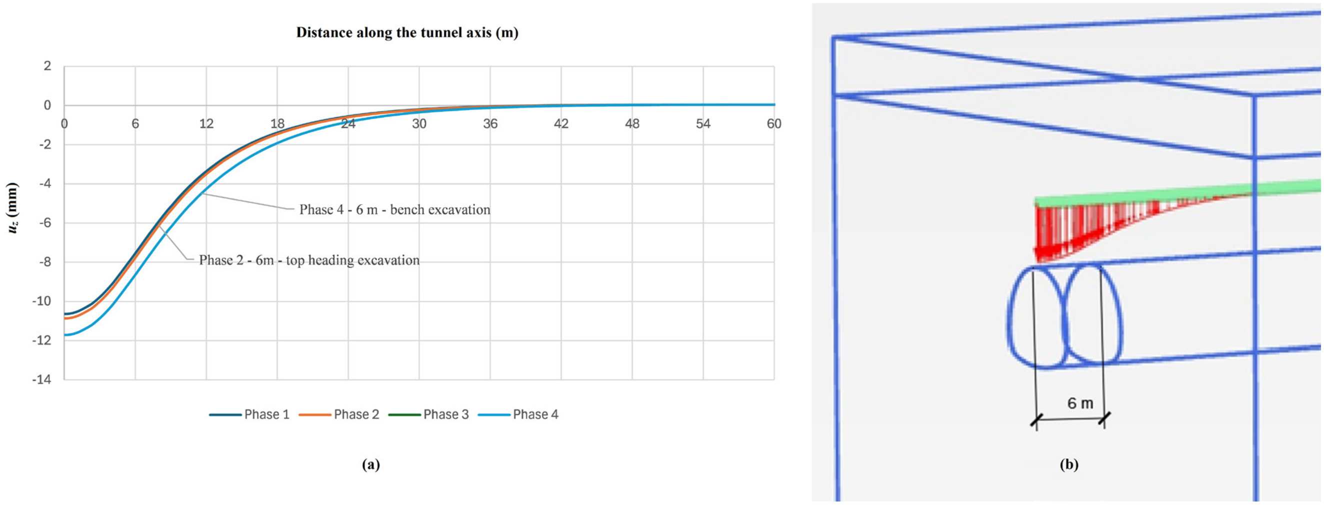

Fig. 8 Settlement of the tunnel crown point at 6 m from the excavation face: (a) longitudinal section along the tunnel axis; (b) 3D view of the tunnel face excavation with ring closure

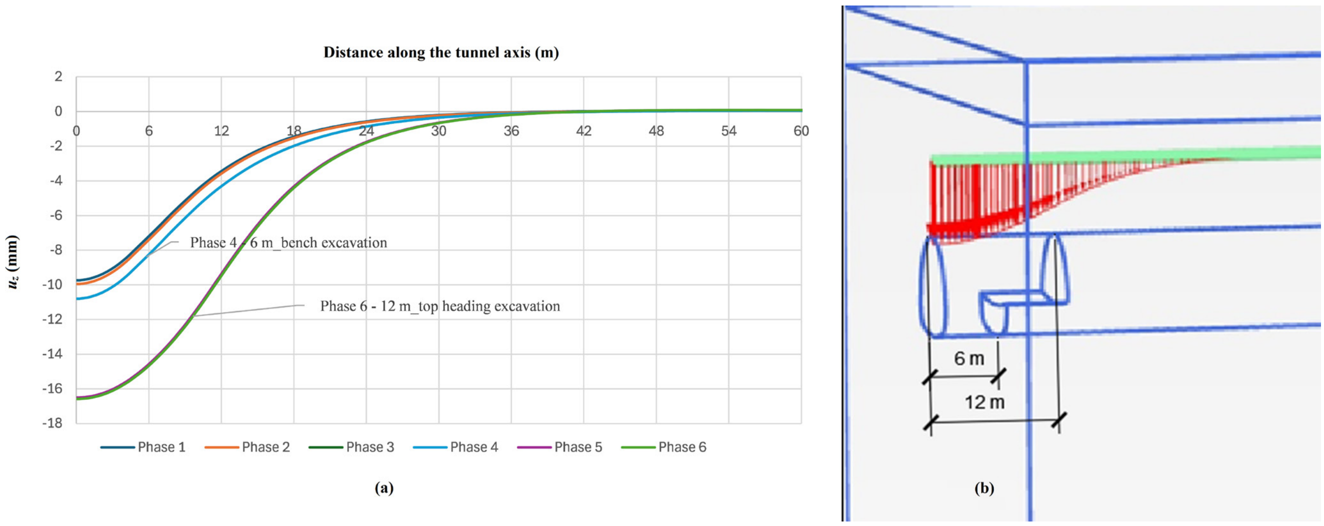

Fig. 9 Settlement of the tunnel crown point at 12 m from the excavation face: (a) longitudinal section along the tunnel axis; (b) 3D view of the tunnel face excavation with ring closure

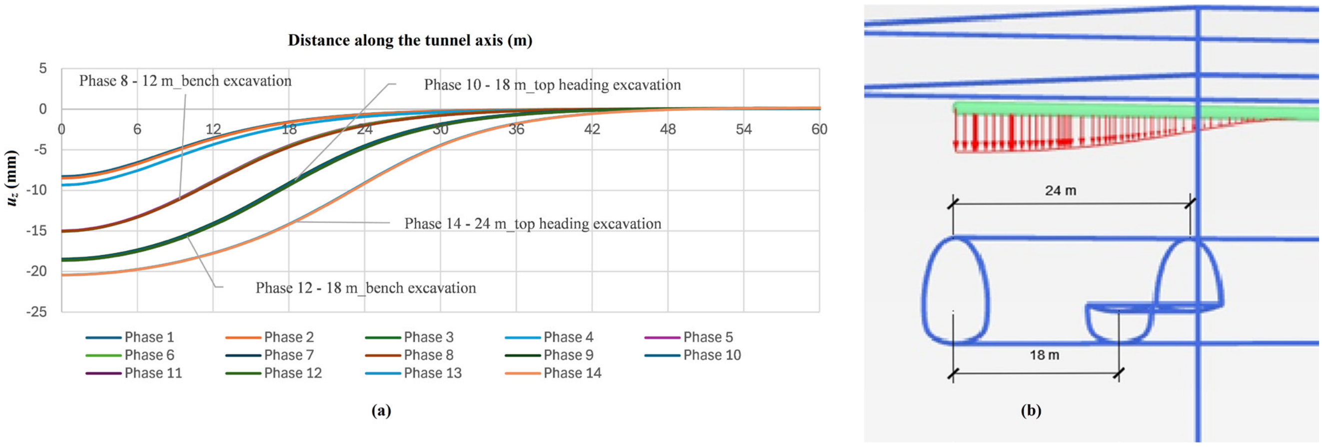

Fig. 10 Settlement of the tunnel crown point at 24 m from the excavation face: (a) longitudinal section along the tunnel axis; (b) 3D view of the tunnel face excavation with ring closure

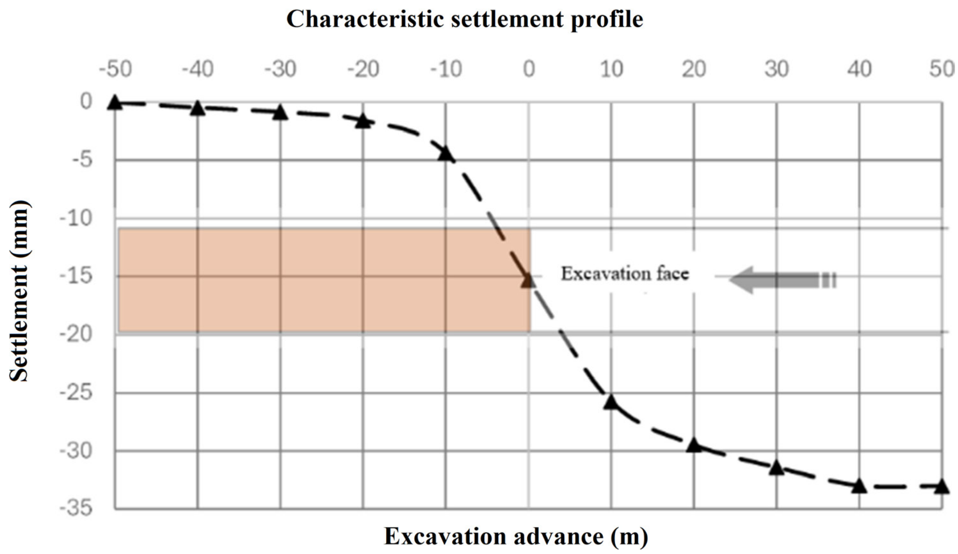

Fig. 11 Typical longitudinal settlement profile for tunnel excavation in marl [35]

observed section of the tunnel. As a result, the diagram of Fig. 12 shows four curves constructed based on the collected convergence data obtained both from the numerical model and from the geodetic measurements.

The curves labeled as phases 1 and 2 respectively represent the settlement of the crown point of the tunnel after the excavation of the tunnel crown and the bench. These values were obtained from numerical models. The other two curves, labeled as phases 3 and 4, represent the settlement after the excavation of the crown and the bench, derived from continuous geodetic measurements conducted during the construction works.

In Table 2, the numerical values of the settlements at the crown points of the tunnel crown section are presented for different distances from the excavation face. Phases 1 and 2 represent the settlements obtained from the numerical model calculations in the Plaxis 3D software [12], while phases 3 and 4 represent the values obtained from geodetic monitoring.

4 Discussion

It can be stated that, in the case of adhering to the construction technological sequences prescribed in the Geotechnical Mission, the shape of the settlement curve obtained corresponds approximately to the shape derived from the numerical models. Geodetic measurements showed greater settlements compared to the numerical models, with deviations ranging from 18% to 24% (Table 3). Nevertheless, the total displacements remained within the theoretically expected limits for marlstone. The magnitude of the settlements ranged between 10 and 30 mm. Furthermore, it can be observed that the smallest deviations were recorded at a distance

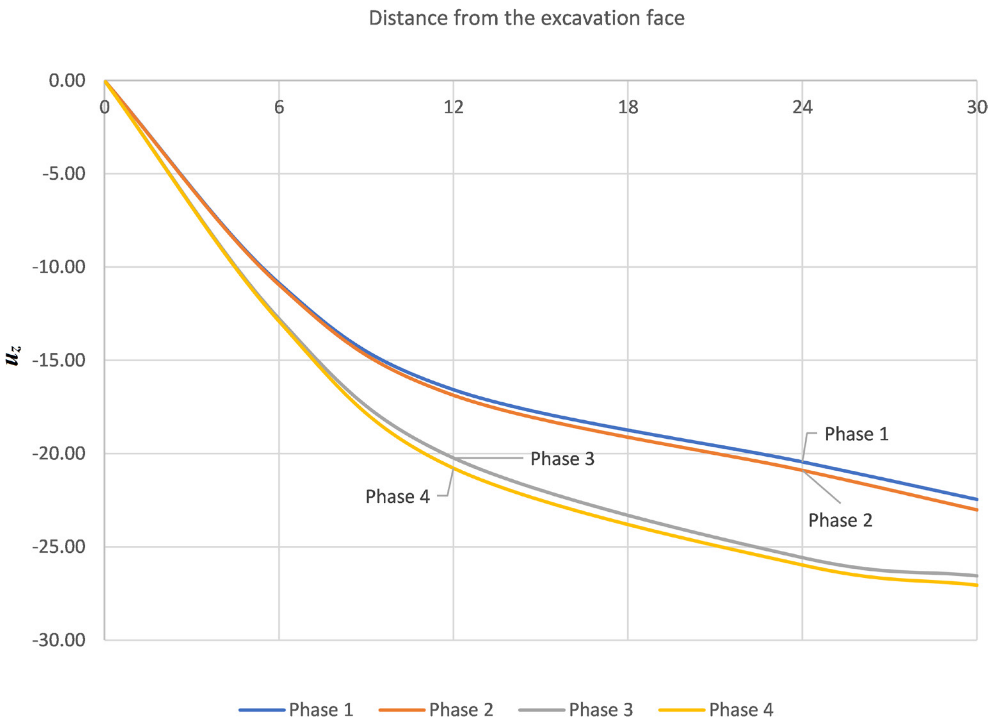

Fig. 12 Settlement of the crown point of the tunnel face section for different distances from the excavation face

Table 2 Settlement of the crown point of the tunnel face section for different distances from the excavation face – numerical model *vs.* survey measurements

Distance from the excavation face (m)	Settlement values u_z (mm)					
	Phase 1 (excavation of the tunnel crown section)	Phase 2 (excavation of the bench)	Relative difference Phase 1 – Phase 3 (%)	Phase 3 (excavation of the tunnel crown section)	Phase 4 (excavation of the bench)	Relative difference Phase 2 – Phase 4 (%)
	Numerical model			Geodetic measurements		
0	0.00	0.00		0.00	0.00	
6	−10.86	−10.95	17.50	−12.76	−12.90	17.81
12	−16.58	−16.88	22.03	−20.23	−20.78	23.14
24	−20.45	−20.90	25.04	−25.57	−25.97	24.26
30	−22.46	−23.02	18.21	−26.55	−27.05	17.51

Table 3 Deviations between numerical model and survey measurements

Distance from the excavation face (m)	Phase 2 (excavation of the bench)	Phase 4 (excavation of the bench)	Difference between geodetic measurements and numerical model (%)
0	0.00	0.00	0.00
6	−10.95	−12.90	17.81
12	−16.88	−20.78	23.14
24	−20.90	−25.97	24.26
30	−23.02	−27.05	17.51

of 30 m between the excavation face and the monitored crown point of the tunnel. This finding is also consistent with the data presented in the characteristic settlement curve for marly materials, where settlement stabilization is observed after a certain distance from the excavation face, i.e., where the values asymptotically approach a constant level. In contrast, the largest deviations were recorded at a distance of 24 m between the excavation face and the monitored crown point of the tunnel, amounting to 24.26%.

These deviations are certainly, at least partially, a result of a number of simplifications made during the development of the numerical model, reflected in the idealization of materials, three-dimensional simplifications, and limitations in mesh element size – all of which are, in turn, constrained by the configuration of the computer equipment available for conducting highly complex and time-consuming numerical analyses.

To further quantify the differences between the numerical model and the geodetic measurements, a basic statistical analysis of the deviations presented in Table 3 was carried out. For this purpose, two standard metrics were calculated: the Root Mean Square Error (RMSE) [36] and the standard deviation of the differences.

The Root Mean Square Error (RMSE) is defined by the following expression (Eq. (2)):

$$\mathrm{RMSE} = \sqrt{\frac{1}{n}\sum_{i=1}^{n}\left(x_i - y_i\right)^2}, \quad (2)$$

where x_i are the settlement values obtained from the numerical model, y_i are the values from the geodetic measurements, and n is the number of observed points. Based on the data presented in Table 3, the RMSE is:

$$\mathrm{RMSE} \approx 3.71 \text{ mm}.$$

The standard deviation [37] of the differences is calculated according to the following expression (Eq. (3)):

$$\sigma = \sqrt{\frac{1}{n}\sum_{i=1}^{n}\left(d_i - d\right)^2}, \quad (3)$$

where di is the individual difference between the model and the measurements, and d is their mean value. The obtained standard deviation is:

$$\sigma \approx 1.21 \text{ mm}.$$

The obtained values indicate consistent deviations between the numerical predictions and the actual deformations, where the RMSE confirms the presence of a systematic error in the prediction, while the low standard deviation indicates the stability of deviations at the analyzed points. These results further confirm the need for dynamic updating of the numerical model in accordance with field data, thereby improving the reliability of deformation response predictions for the rock mass under real tunneling conditions.

In addition to conventional numerical updating, various advanced forecasting models have been proposed in the literature to improve defromation prediction accuracy.

Also, in literature different models for forecasting of deformations could be fined based on grey-stochastic simulation and autoregressive process [38], multivariate singular spectrum analysis [39], deep learning [40], grey theory [41, 42], generalized regression neural network [43], support vector machine [44]. Implementation of data obtained from field measurements in construction phase of the underground projects gathered with precise measuring instruments can help with better organization of construction site as well as planning the maintenance of underground roadways more efficiently.

A similar need for dynamically updating the numerical model based on field deformations was also confirmed in the case of the Ibarac Tunnel, where numerical analysis was used to define remedial measures after a lining collapse in a parking niche [45].

Regarding material idealization, it should be noted that soil, as a medium, is a heterogeneous material, which is simplified in the Plaxis 3D software [12] package by using average characteristic values. In this way, a certain degree of soil homogenization is achieved. Furthermore, as was the case in this model, a single effective value of the shotcrete elastic modulus is often used, representing the average stiffness during the critical loading phase. In addition, during the construction process itself, deviations may occur due to various factors, which can ultimately lead to increased convergence values.

The results confirm the need for dynamic updating of numerical models in accordance with field measurements, thereby enhancing the application of the observational method under real tunneling conditions.

5 Conclusions

The analysis of the behavior of the Kobilja Glava tunnel structure was carried out by combining three-dimensional numerical modeling and geodetic monitoring under real construction conditions. The obtained results showed that the numerically calculated settlement pattern largely corresponds to the actually measured values, with deviations remaining within acceptable limits for marl rock mass. This confirms the technical validity of the applied model and the designed support system.

Geodetic measurements indicated systematically greater settlements compared to the numerical predictions, with deviations ranging from 18% to 24%, the largest difference being recorded at a distance of 24 m from the excavation face. Nevertheless, the total displacements remained within theoretically expected values, and the closure of the excavation ring demonstrated a stabilizing effect on deformations, consistent with the behavior of rock mass in weakly consolidated marls. These deviations point to model limitations related to material idealization, neglecting the time-dependent stiffness of shotcrete, and simplified boundary conditions.

Based on the conducted research, recommendations for further methodological development are directed toward improving monitoring, modeling, and input parameter definition. It is necessary to integrate advanced technologies such as 3D laser scanning, satellite interferometric techniques (InSAR), and geophysical methods for precise characterization of the rock mass damage zone, which would significantly enhance the reliability of geotechnical monitoring. At the same time, it is recommended to establish an adaptive framework in which numerical models are continuously updated based on field data, allowing for dynamic integration of predictions and actual measurements, as well as more efficient control of structural stability. Additionally, it is essential to expand laboratory and in-situ testing, including the rheological characteristics of shotcrete, in order to improve the accuracy of numerical discretization and reduce the model's sensitivity to simplifications that may affect result accuracy.

References

[1] Niu, G., He, X., Xu, H., Dai, S. "Tunnelling-induced ground surface settlement: A comprehensive review with particular attention to artificial intelligence technologies", Natural Hazards Research, 4(1), pp. 148–168, 2024. https://doi.org/10.1016/j.nhres.2023.11.002

[2] Filipović, S., Bektašević, E., Gutić, K., Musa, N., Sakić, N. "Research on the phenomenon of increasing borehole diameter at the installation of rod anchors in marl using wet technology compared to dry drilling procedure", Global Journal of Engineering and Technology Advances, 22(02), pp. 001–014, 2025. https://doi.org/10.30574/gjeta.2025.22.2.0019

[3] Hrestak, T., Jaguljnjak Lazarević, A., Frgić, L. "Stress and strain analysis during the Sleme tunnel excavation", Tehnički Vjesnik, 22(3), pp. 703–709, 2015. https://doi.org/10.17559/TV-20140530103847

[4] Bektašević, E., Filipović, S., Gutić, K., Musa, N. "Defining the optimal distance between technological sequences during tunnel excavation in poor rock mass", e-ZBORNIK, 14(28), pp. 47–57, 2024. https://doi.org/10.47960/2232-9080.2024.28.14.47

[5] Bektašević, E., Mušija, A., Gutić, K., Sakić, N. "Application of seismic refraction for determining geomechanical parameters in the excavation zone of the Vranduk Tunnel on the Corridor Vc route", In: International Conference Synergy of Architecture and Civil Engineering (SINARG 2025), Niš, Serbia, 2025, pp. 513–524. ISBN 978-86-82810-16-2 https://doi.org/10.62683/SINARG2025.065

[6] Bektašević, E., Strelec, S., Sakić, N., Gutić, K. "Multichannel surface wave analysis in the context of shallow geophysical investigations", Academia Engineering, 2(3), pp. 1–18, 2025. https://doi.org/10.20935/AcadEng7876

[7] Sharifzadeh, M., Kolivand, F., Ghorbani, M., Yasrobi, S. "Design of sequential excavation method for large span urban tunnels in soft ground – Niayesh tunnel", Tunnelling and Underground Space Technology, 35, pp. 178–188, 2013. https://doi.org/10.1016/j.tust.2013.01.002

[8] Bektašević, E., Gutić, K., Kadrić, S., Sikira, D. "Deformation analysis during tunnel excavation in poor rock mass", In: 8th International Conference on Road and Rail Infrastructure, Cavtat, Croatia, 2024, pp. 799–806. ISBN 9789771848981 https://doi.org/10.5592/CO/cetra.2024.1514

[9] Bektašević, E., Filipović, S., Gutić, K., Hodžić, D., Musa, N. "Analysis of surface deformations during excavation of a small overburden tunnel in weak rock masses", Journal of the Faculty of Civil Engineering and Architecture, 40(1), pp. 35–48, 2025. https://doi.org/10.62683/ZRGAF40.3

[10] Rokić, L. "Elaborat o inženjerskogeološkim i geotehničkim karakteristikama terena duž trase tunela Kobilja Glava" (Report on the Engineering-geological and geotechnical characteristics of the terrain along the Kobilja Glava Tunnel route), Institute of Geotechnics and Geology, Faculty of Civil Engineering, University of Sarajevo, Sarajevo, Bosnia and Herzegovina, 2011. (in Bosnian)

[11] Milaković, D., Kovačević, M.-S. "Utjecaj iskopa tunela na stabilnost pokosa predusjeka" (Influence of tunnel excavation on the stability of preliminary cross-section slopes), Građevinar, 60(8), pp. 679–685, 2008. [online] Available at: https://urn.nsk.hr/urn:nbn:hr:237:725821 [Accessed: 01 February 2026] (in Croatian)

[12] Bentley Systems "Plaxis 3D, (21)", [computer program] Available at: https://www.bentley.com/software/plaxis-3d/ [Accessed: 15 May 2025]

[13] IRGO Consulting d.o.o., Lotus d.o.o. "Glavni projekt izmjene projekta tunela "Kobilja Glava" na I transverzali, od km 3+420.00 do km 4+180.00, Knjiga D, Mapa D.4- Tunelski iskop" (Main design of the modification of the Kobilja Glava Tunnel project on the First Transversal, from km 3+420.00 to km 4+180.00, Book D, Map D.4 – Tunnel excavation), IRGO Consulting d.o.o., Ljubljana, Slovenia, 2023. (in Bosnian)

[14] Zhao, C., Zhang, X., Alimardani Lavasan, A., Lin, C., Chen, Y. "Numerical Modeling of Soil and Structure Behavior for Tunneling in Different Types of Soil", Buildings, 14(11), 3380, 2024. https://doi.org/10.3390/buildings14113380

[15] Huang, X., Zhang, H., Guo, J., Zhang, Z., Chao, X. "Optimization of Advanced Support Parameters of Surrounding Rock in Tunnels Constructed by ADECO-RS", Buildings, 14(10), 3297, 2024. https://doi.org/10.3390/buildings14103297

[16] Zlatanović, E., Šešov, V., Lukić, D. Č., Bonić, Z. "Influence of a new-bored neighbouring cavity on the seismic response of an existing tunnel under incident P- and SV-waves", Earthquake Engineering & Structural Dynamics, 50(11), pp. 2980–3014, 2021. https://doi.org/10.1002/eqe.3497

[17] Xiao, Z., Wang, J. "A Three-Dimensional Model of Shield Tunnel considering Interaction of Soil and Lining", Mathematical Problems in Engineering, 2022(1), 4245384, 2022. https://doi.org/10.1155/2022/4245384

[18] Bektašević, E., Antičević, H., Gutić, K., Sikira, D. "Application of seismic methods for determining the depth of the rock mass damage zone around the excavation profile by blasting", Global Journal of Engineering and Technology Advances, 18(03), pp. 139–151, 2024. https://doi.org/10.30574/gjeta.2024.18.3.0051

[19] Bektašević, E., Antičević, H., Gutić, K., Sikira, D. "Određivanje dubine zone oštećenja stijenske mase oko profila iskopa miniranjem seizmičkom cross-hole tomografijom u tunelu "Šubir" na autocesti zagreb-split" (Determination of the depth of the rock mass damage zone around the excavation profile by blasting with seismic cross-hole tomography in the "Šubir" tunnel on the Zagreb-Split motorway), Nauka+Praksa, 27(1), pp. 13–19, 2024. (in Croatian) https://doi.org/10.62683/nip27.13-19

[20] Equihua-Anguiano, L. N., Viveros-Viveros, F., Pérez-Cruz, J. R., Chávez-Negrete, C., Arreygue-Rocha, E., Orozco-Calderón, M. "Displacement nomograph from two (2D) to three (3D) dimensions applied to circular tunnels in clay using finite element", In: Proceedings of the 19th International Conference on Soil Mechanics and Geotechnical Engineering, Seoul, South Korea, 2017, pp. 733–736. ISBN XXXX [online] Available at: https://www.issmge.org/uploads/publications/1/45/06-technical-committee-03-tc103-10.pdf [Accessed: 01 February 2026]

[21] Niu, G., He, X., Xu, H., Dai, S. "Development of Rock Classification Systems: A Comprehensive Review with Emphasis on Artificial Intelligence Techniques", Eng, 5(1), pp. 217–245, 2024. https://doi.org/10.3390/eng5010012

[22] Rocscience Inc. "RocLab, (1.0)", [computer program] Available at: https://www.rocscience.com/software/roclab [Accessed: 15 May 2025]

[23] Hemeda, S. "Geotechnical modelling and subsurface analysis of complex underground structures using PLAXIS 3D", International Journal of Geo-Engineering, 13(1), 9, 2022. https://doi.org/10.1186/s40703-022-00174-7

[24] Wu, D., Chen, X., Tao, Y., Meng, X. "Estimating Mohr–Coulomb Strength Parameters from the Hoek–Brown Criterion for Rock Slopes Undergoing Earthquake", Sustainability, 15(6), 5405, 2023. https://doi.org/10.3390/su15065405

[25] Mohyla, M., Vojtasik, K., Hrubesova, E., Stolarik, M., Nedoma, J., Pinka, M. "Approach for Optimisation of Tunnel Lining Design", Applied Sciences, 10(19), 6705, 2020. https://doi.org/10.3390/app10196705

[26] Li, Z., Diao, P., Lu, W., Zhang, Y. "Performance of Single-Layer Lining Using Shotcrete and Reinforcement Ribs Employed for Supporting Large-Span Tunnel", Materials, 16(24), 7590, 2023. https://doi.org/10.3390/ma16247590

[27] Autodesk "AutoCAD, (2024)", [computer program] Available at: https://www.autodesk.com/products/autocad/overview [Accessed: 15 May 2025]

[28] Goel, R. K. "Monitoring of Deformation and Assessment of Support During Tunnel Excavation", Journal of Rock Mechanics and Tunnelling Technology (JRMTT), 28(2), pp. 103–119, 2022. [online] Available at: https://www.researchgate.net/publication/388572309_Monitoring_of_Deformation_and_AssessmentTunnel_Excavation [Accessed: 01 February 2026]

[29] Lienhart, W. "Geotechnical monitoring using total stations and laser scanners: critical aspects and solutions", Journal of Civil Structural Health Monitoring, 7(3), pp. 315–324, 2017. https://doi.org/10.1007/s13349-017-0228-5

[30] Singh, S. K., Banerjee, B. P., Raval, S. "Three dimensional unique identifier based automated georeferencing and coregistration of point clouds in underground environment", [preprint] arXiv, arXiv:2102.10731, 22 February 2021. https://doi.org/10.48550/arXiv.2102.10731

[31] FM Inženjering d.o.o. "Geotehnička misija G21. Dopunski dio glavnog projekta tunela Kobilja glava" (Geotechnical Mission G21. Supplementary part of the Main Design of the Kobilja Glava Tunnel), [unpublished project documentation] FM Inženjering d.o.o., Sarajevo, Bosnia and Herzegovina, 2021. (in Bosnian)

[32] Suárez-Fino, J. F., Mayoral, J. M. "Numerical Modeling for Tunnel Lining Optimization", Applied Sciences, 14(16), 7415, 2024. https://doi.org/10.3390/app14167415

[33] Kontogianni, V., Stiros, S. "Tunnel monitoring during the excavation phase", presented at 11th FIG Symposium on Deformation Measurements, Santorini, Greece, May 5–28, 2003. [online] Available at: https://www.fig.net/resources/proceedings/2003/santorini_comm6/F-Tunnels/F3.pdf [Accessed: 01 February 2026]

[34] Perazzelli, P., Rotonda, T., Boldini, D., Ajmone-Cat, A. M., Gianvecchio, P. M. "Analysis of convergence data and 3D numerical modelling of tunnels excavated in fine-grained soils", In: Viggiani, G. (ed.) Geotechnical Aspects of Underground Construction in Soft Ground, CRC Press, 2012, pp. 281–289. ISBN 978-0-415-68367-8 [online] Available at: https://www.research-collection.ethz.ch/server/api/core/bitstreams/af9b16a7-2ded-42ad-8549-3e989e02badd/content [Accessed: 01 February 2026]

[35] Chen, Y., Geng, X., Li, J., Zhang, M., Zhu, C., Cai, M., Zhao, W., Zhou, X., Wang, T. "Excavation method optimization and mechanical responses investigating of a shallow buried super large section tunnels: A case study in Zhejiang", Scientific Reports, 14(1), 6281, 2024. https://doi.org/10.1038/s41598-024-56982-7

[36] Hodson, T. O. "Rootmeansquare error (RMSE) or mean absolute error (MAE): when to use them or not", Geoscientific Model Development, 15, pp. 5481–5487, 2022. https://doi.org/10.5194/gmd-15-5481-2022

[37] Wackerly, D. D., Mendenhall, W., Scheaffer, R. L. "Mathematical Statistics with Applications", Brooks/Cole, 2008. ISBN 978-0-495-11081-1

[38] Crnogorac, L., Lutovac, S., Tokalić, R., Gligorić, M., Gligorić, Z. "Steel Arch Support Deformations Forecast Model Based on Grey–Stochastic Simulation and Autoregressive Process", Applied Scienes, 13(7), 4559, 2023.
https://doi.org/10.3390/app13074559

[39] Crnogorac, L., Tokalić, R., Gligorić, Z., Milutinović, A., Lutovac, S., Ganić, A. "Gate Road Support Deformation Forecasting Based on Multivariate Singular Spectrum Analysis and Fuzzy Time Series", Energies, 14(12), 3710, 2021.
https://doi.org/10.3390/en14123710

[40] Luo, X., Gan, W., Chen, Y., Ma, E. "A Deep Learning Prediction Model for Structural Deformation Based on Temporal Convolutional Networks", Computational Intelligence and Neuroscience, 2021(1), 8829639, 2021.
https://doi.org/10.1155/2021/8829639

[41] Rao, J., Tao, Y., Xiong, P., Nie, C., Peng, H., Xue, Y., Xi, Z. "Research on the large deformation prediction model and supporting measures of soft rock tunnel", Advances in Civil Engineering, 2020(1), 6630546, 2020.
https://doi.org/10.1155/2020/6630546

[42] Xiong, X. "Research on Grey System Model and Its Application on Displacement Prediction in Tunnel Surrounding Rock", The Open Mechanical Engineering Journal, 8, pp. 514–518, 2014.
https://doi.org/10.2174/1874155X01408010514

[43] Yu, Sun, Hongzhen, Z., Yanna, C. "Application of GRNN in Time Series Prediction for Deformation of Surrounding Rocks in Soft Rock Roadway", In: 2011 Fourth International Conference on Intelligent Computation Technology and Automation, Shenzhen, China, 2011, pp. 63–66. ISBN 978-1-61284-289-9
https://doi.org/10.1109/ICICTA.2011.23

[44] Yao, B.-Z., Yang, C.-Y., Yao, J.-B., Sun, J. "Tunnel surrounding rock displacement prediction using support vector machine", International Journal of Computational Intelligence Systems, 3(6), pp. 843–852, 2010.
https://doi.org/10.2991/ijcis.2010.3.6.14

[45] Kadrić, S., Bektašević, E., Gutić, K., Sikira, D. "Numeričke analize stabilnosti iskopa tunela Ibarac i stabilizacija urušenog dijela, parking niše" (Numerical analysis of the stability of the Ibarac tunnel excavation and stabilization of the collapsed part, parking niche), Nauka+Praksa, 26, pp. 1–10. (in Croatian)